ELSEVIER

Journal of Nuclear Materials 241–243 (1997) 988–992

journal of nuclear materials

Locked modes induced plasma–wall interactions in RFX

M. Valisa *, T. Bolzonella, L. Carraro, E. Casarotto, S. Costa, L. Garzotti, P. Innocente, S. Martini, R. Pasqualotto, M.E. Puiatti, R. Pugno, P. Scarin

Gruppo di Padova per Ricerche sulla Fusione, Corso Stati Uniti 4, I-35127 Padua, Italy

Abstract

In the RFX reversed field pinch ($R = 2$ m, $a = 0.45$ m) the plasma–wall interaction has been characterised in all of the discharges by the presence of the locking both in phase and in the laboratory frame of unstable MHD modes. These locked modes cause a helical deformation of the magnetic surfaces driving large power fluxes onto the wall. The plasma edge is severely perturbed: a power density loading as high as 100 MW m^{-2} may locally be exceeded, the surface of the plasma facing components reach the sublimation temperature, the impurity release and the power radiated locally increase by a factor of ~ 100, large fluctuations in the electron density develop and halo currents flow in the inconel vacuum vessel. It is estimated that the locked modes are responsible for losses that may amount to up to about 30% of the total power input.

Keywords: RFX; Reversed field pinch; Impurity source; Energy balance

1. Introduction

The control of the interaction of magnetically confined plasmas with the first wall is a key issue in thermonuclear fusion experiments. Several tokamaks have demonstrated the importance of minimising the impurity production and controlling the recycling of the fuelling gas in order to obtain enhanced confinement modes [1]. Analogous conclusions have been drawn in reversed field pinch (RFP) configurations where wall conditioning procedures lead to an improved performance [2,3]. In RFP's the edge region plays a crucial role in the confinement properties of the plasma, being characterised by relatively well defined magnetic surfaces in contrast with the plasma core, where the presence of overlapping magnetic islands implies a large degree of field line stochasticity and ultimately an enhanced radial transport [4,5]. Moreover, in the RFP edge a dynamo-like process generates a large parallel current density to sustain the toroidal magnetic flux and therefore a low plasma resistivity is a premium [6].

In RFX the presence of locked MHD modes in all of the discharges results in a large kink perturbation that leads to a strong enhancement of the plasma–wall interaction. This paper describes the phenomenology associated with such perturbation and analyses the related impact on the confinement properties of the plasma.

2. The RFX experiment

The plasma facing components in RFX are constituted by 2016 graphite tiles (10×18 cm^2) which protect the inconel vacuum vessel almost completely, with only a 1 cm interspace left between them. The protection has been quite effective and the concentration of metals in the plasma has never significantly contributed to Z_{eff}, though evidence of erosion by direct power deposition and arc formation on the vessel has been found. No limiters are present and the plasma should lean evenly onto the first wall. As a matter of fact the presence of errors in the magnetic configuration introduces asymmetries in the plasma–surface interaction. The vacuum vessel is made by two nested inconel sheets 2 and 1 mm thick, respectively, separated by 20 mm and strengthened by internal inconel corrugations and 72 poloidal rings onto which the tiles are fixed. A 5 cm thick aluminium shell surrounds the vessel at $b/a = 1.17$ with the purpose of stabilising MHD modes. The shell has two poloidal and two toroidal gaps. Recently one poloidal and the external toroidal gaps have been short-circuited to reduce the associated field errors.

* Corresponding author. Tel.: +39-49 8295 031; fax: +39-49 8700 718; e-mail: valisa@pdigi3.igi.pd.cnr.it.

PII S0022-3115(96)00645-9

3. The locked modes in RFX

The progressive reduction of the field errors to a few percent of the local poloidal field (the dominant component at the edge of an RFP), especially those generated by the gaps in the conductive shell, has not been sufficient to eliminate the wall locking of MHD modes in RFX yet. These locked modes develop during the formation phase of the reversed field configuration and lock in phase as soon as the toroidal field reversal is reached.

The resulting magnetic perturbation (referred to as LMP for locked mode perturbation) is made up of a spectrum of $n = 7–15$, $m = 1$ modes phase-locked between themselves and to the wall [7] and is seen as a helical deformation of the plasma with amplitude peaked at the position of maximum in-phasing of the modes. The LMP position is detected by two toroidal arrays of 72 toroidal magnetic field pickup coils at a poloidal angle of 20.5° and 200.5°, respectively. In Fig. 1a the time average over a 10 ms interval of the toroidal profile of the $m = 1$ perturbation derived from the two arrays is shown for a pulse where the LMP position was at $\Phi = 65°$. The $m = 1$ helical shape of the LMP is inferred also from the local horizontal and vertical shift of the last plasma surface, measured around the torus by 6 poloidal arrays of pick-up coils and by the electron density profile measured by an 8-chord interferometer. The maximum radial displacement of the plasma due to the LMP is ≈ 2 cm, and decays by more than 50% in half the typical toroidal period of 30°–35°. The modes producing the perturbation are resonant internally (at $r/a = 0.6 \div 0.9$) relative to the surface of toroidal field reversal (at $r/a \approx 0.9$) and cause at the wall an helical band of interaction. The effect is similar to an helical limiter performing 1–2 poloidal turns on a toroidal angle of 30–35° each. The helical footprint on the first wall forms an angle of 30° relative to the local magnetic field line and may be seen (for the same shot) in Fig. 1b that shows a tangential view taken by a CCD camera from an equatorial port. The interaction appears to be concentrated at the edge of the tiles and at the protection caps of the clamping keys (at the centre of the tiles) where the tile surface is almost perpendicular to the incoming flux that is nearly poloidal, with a radial component due to the local radial shift of the plasma column and to the local field error.

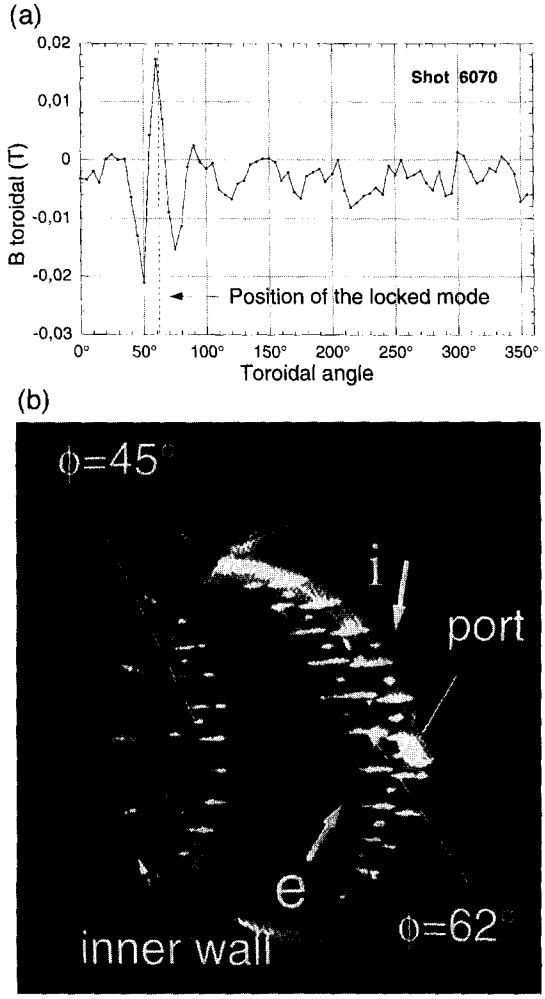

Fig. 1. (a) Profile of the $m = 1$ toroidal field perturbation, averaged over 10 ms, derived from the arrays of pick-up coils for shot 6070. (b) Footprints of the $m = 1$ perturbation on the external side of the wall in the shot 6070 as seen by a CCD camera equipped with a plastic red filter. The two regions of enhanced interaction correspond to the helical form of the perturbation shown in (a). The directions of the electron and ion drifts are also shown.

3.1. Asymmetries

Due to the LMP-induced plasma surface distortion the ion and electron flows along the magnetic field lines are separately intercepted by the wall. This can be seen in Fig. 2 showing a C II image (taken with an interference filter centred at 5150 ± 40 Å, corresponding to a metastable state transition), where the electron drift (flowing almost poloidally from bottom to top) and the ion drift (from top to bottom) define two distinct footprints in the region of interaction: the electrons hit the trailing edge of the tiles, while the ions hit the leading ones. The flow along the electron drift side is dominated by the presence of the so called fast electrons: a tail in the energy distribution of the electrons with an equivalent temperature of 200 eV as measured by an electron energy analyser [8], much higher than the local temperature of 10–20 eV.

The toroidal width of the interaction zone is typically 20–60 cm with the largest values at the highest plasma currents.

3.2. Effects on density

When any of the interferometer chords crosses directly the LMP plasma–wall helical interaction, enhancements of

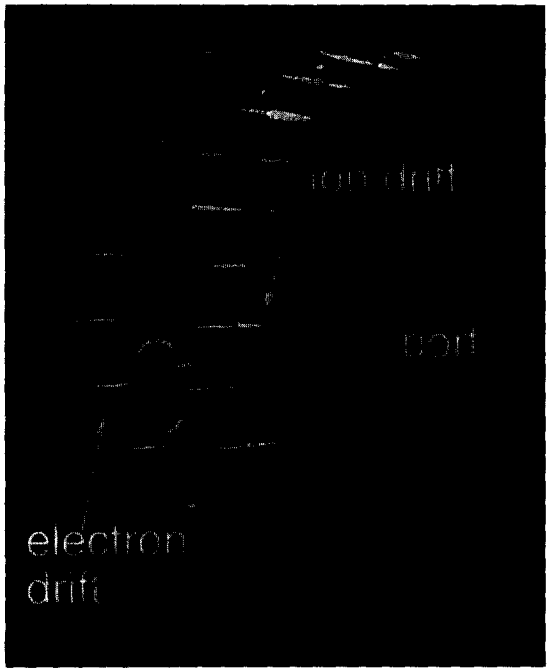

Fig. 2. A CCD image taken with a C II filter showing some details of the plasma–wall interaction associated to a LMP. The particle fluxes are almost poloidal and hit preferentially the edges of the tiles.

density and density fluctuations are measured (Fig. 3). The amplitude of the fluctuations is as large as 0.5×10^{20} m^{-2} peak-to peak in line-integral density units, which is $30 \div 50$ times larger than the typical values outside the LMP region. The enhanced fluctuations are seen only by chords directly striking the LMP helix, or when they are less than 20–30 cm away from it moving along magnetic field lines in the electron drift direction. This implies that actually the enhanced fluctuations occur in the shadow of the LMP 'virtual' limiter. Taking into account that the radial perturbation of the last plasma surface caused by the LMP is estimated to be ≈ 2 cm, one may infer that the thickness of the enhanced fluctuation region crossed by the interferometer chords is also ≈ 2 cm, implying that the average and the fluctuating density are in the 10^{21} m^{-3} range. Consistent with the observation of highly localised phenomena, the power spectrum of the enhanced fluctuations is broader than normal and only $20 \div 30\%$ of the power is contained in the interval $0 \div 5$ kHz. The decrease with frequency is nearly linear so that the power density decreases of one order of magnitude in the interval 5–50 kHz.

The large amplitude and edge localisation of the density fluctuations suggest that they are due to the continual ionisation and loss of neutral atoms coming from the wall. In fact, computing a particle influx/outflux balance from the time derivative of the fluctuating density, influxes in the 10^{23} m^{-2} s^{-1} range are inferred. These values are comparable to the graphite thermal sublimation influxes evaluated at the 'hot spots' by CCD cameras.

3.3. Impurity release

The mode locking to the wall cause a large increase of the impurity influx. The CCD equipped with a filter centred around the C II line at 5150 Å, shows that the carbon-influx may vary from $1–5 \times 10^{19}$ to more than 10^{22} m^{-2} s^{-1}. These values are inclusive of the contribution from the ground state of C II experimentally determined by means of filter monitors coupled to photomultipliers and are based on the assumption that the electron temperature at the edge is not affected by the locking. This approximation may result in an uncertainty on the influx values as high as a factor of 2. At the hot spots, where influx values larger than 10^{23} m^{-2} s^{-1} are obtained, the measurements should be deconvolved from the contribution of the thermal radiation, that in most of the cases may dominate the signal and are not considered here. Integrating the flux over the LMP area one may show that the associated carbon influx in many circumstances can be more than 50% of the total one.

Hydrogen, oxygen and carbon filter monitors coupled to telescope lenses and photomultiplier detectors [9] confirm that in conjunction with the LMP the carbon influx may experience an enhancement of a factor 100–200 while for oxygen the enhancement factor is 30–70 and 20–50 for hydrogen.

3.4. Blooming

Infrared CCD observations (1040 ± 5 nm) in proximity of the LMP show that the edge of the carbon tiles easily exceed 2000°C and that at high currents (0.8–1 MA), values close to the sublimation temperature may be reached (3350°C). This results in carbon blooming processes that

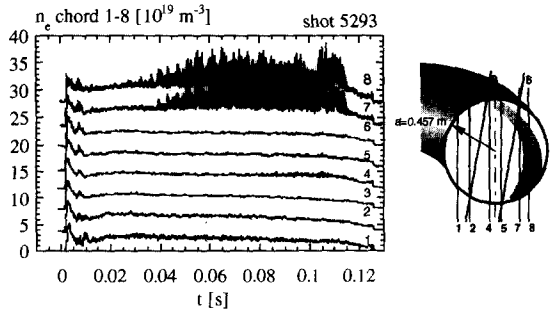

Fig. 3. Line averaged densities (in 10^{19} m^{-3} units) from the CO_2 interferometer. The enhanced fluctuations are seen on the two outermost chords. A schematic shows the position of the eight chords and the region of plasma wall interaction in the poloidal section.

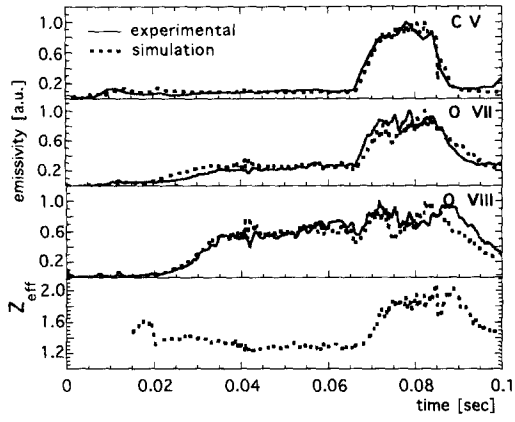

Fig. 4. Behaviour of C V, O VII and O VIII emissivities in a shot with blooming occurring at ≈ 65 ms. The result of a 1D simulation and the calculated Z_{eff} are also shown. Z_{eff} experiences an enhancement of ≈ 50% from 1.3 to 2.

appear as a sudden increase of the local influx and of the average concentration of carbon, together with a similar enhancement in the total radiation and also in the oxygen emissivities. The consequent increase in Z_{eff} and in density causes an increase of the loop voltage and a premature decay of the plasma current [10]. The process typically saturates and the reduction of the plasma current with the consequent variation of the plasma column equilibrium leads to a slight modification of the locking position and to the drop of the local surface temperature. Fig. 4 shows an example of a 1 MA discharge where the phenomenon occurs at $t \approx 65$ ms. The experimental C V, O VII O VIII emissivities have been simulated by a 1D collisional-radiative impurity transport model, indicating that a Z_{eff} increase from 1.3 up to 2 is caused by the blooming.

3.5. Power dissipation

From the surface temperature measurements one may deduce the power dissipated by parallel transport due to the presence of the LMP. Using for simplicity the semi-infinite model the power density P dissipated onto the wall may be related to the surface temperature T (in K) of the tile by the simple relation $T = 2P\xi^{-1/2}(t)^{1/2}$ where $\xi = \rho\lambda c$ (ρ is the density, λ the thermal conductivity and c is the specific heat) and t is time [11]. The power dissipated at the hot spots in high current discharges may exceed 100 MW m^{-2}. By considering the images taken in the same shot from three CCD cameras one may estimate the total area covered by the hot spots, that is typically of the order of ≈ 1000 cm^2. The total power dissipated on the hot spots associated with a locked mode is of the order of 3 to 5 MW, that is 10 to 15% of the total power input (the ohmic input in RFX is in fact 20–30 MW, due to the high anomalous resistivity). It should be emphasised that this value is underestimated because of the small dynamic range of the CCD cameras. Moreover the latter cannot detect temperatures below 600°C and any effects causing temperature variations below that threshold is completely neglected.

3.6. Total radiation

The bolometer signals typically saturate when the LMP occurs at its toroidal position. On the other hand the emission spectrum detected by a survey spectrometer and wavelength integrated from 100 to 1100 Å increases more than one hundred times in presence of the LMP. Taking the typical spatial extension of the phenomenon into account this indicates that the power locally radiated because of the LMP is at least 50% of the total radiated one.

3.7. Halo currents

The tiles and the inconel vessel may short-circuit the field lines intercepted by the wall generating halo currents [12]. From the estimates of the power dissipated on the edges of the graphite tiles (P_{diss}) and considering the fast electrons equivalent temperature of ≈ 200 eV, one may deduce that a current I_{halo} of P_{diss}/T_e (eV) ≈ 25 kA may flow through the vessel. The pitch of the perturbation is such that potential differences could develop both along the poloidal stiffening rings or between two of them or even across single tiles. The halo current would find its way where the path is less resistive. Considering the contact resistance between tile and vessel, a power dissipation greater than 1.5 MW can be estimated, consistent with the one deduced by thermal measurements on the liner by means of arrays of thermocouples and with the evidences of damages at the tile-vessel interfaces that have been ascribed to current flows higher than 3 kA [13].

3.8. Helicity dissipation

The interception of magnetic field lines with the wall may be associated with a loss of magnetic helicity [14] and ultimately with an increase in the toroidal loop voltage. Following the model described in [14] the loop voltage increase may be expressed as $\Delta V \approx \Delta\chi(\Theta/\pi a^2)A$, where Θ is the pinch parameter $(B_\theta(a)/\langle B_z\rangle)$, a is the minor radius of the plasma, A the area intercepting the magnetic field lines and $\Delta\chi = 1.8\ kT_e/e$ the potential drop across the limiter, that is estimated to be ≈ 20–30 V and is consistent with the voltage required to sustain the halo current estimated above. Considering the area A of interaction seen by the CCD cameras a loop voltage enhancement of ≈ 7 V is deduced. This represents a lower limit since the area of field line interception is probably larger. This value is to be compared with the anomalous 10 V that had previously been estimated from Z_{eff} measurements [10].

3.9. Effects on plasma core in the LMP section

The main parameters of the plasma do not show toroidal asymmetries related to the LMP. The electron temperature yielded by a soft X-ray PHA system, which is sensitive to the maximum value along the line of sight, and the ion temperature measured by a time of flight neutral particle analyser are statistically independent on the LMP toroidal position. This is to be ascribed to the large parallel conductivity of the plasma. Slight dependencies have been found in the C V and C VI emissions as a consequence of the large carbon influx enhancement. A dependence on the LMP position has also been found in the ratio between the resonant ($1s^2$–$1s2p\ ^1S_0$–$^1P_1$) and intercombination ($1s^2$–$1s2p\ ^1S_0$–$^3P_1$) CV lines. The latter ratio may be demonstrated to depend inversely on the electron temperature in the region of existence of C V and directly on the neutral particle density. In the present case both causes should be considered.

4. Discussion and conclusions

The presence of MHD modes locked in phase and in the laboratory frame causes in all of the RFX discharges a large kink of the plasma column. In the region where the wall is intersected by the distorted magnetic surfaces the large power fluxes heat the tiles close to the sublimation temperature, enhance the influxes of carbon by a factor of ≈ 100, of oxygen by a factor of ≈ 40 and of hydrogen by a factor of ≈ 30 and largely increase the local density, with a consequent local radiation loss of ≈ 10–30% of the power input. In high current discharges (0.8–1 MA) carbon blooming often occurs, causing a premature quench of the plasma current and representing an operational limit for the machine.

Due to the separated interception of the electron and ion flows at the wall that behaves like a limiter, large halo currents (≥ 25 kA) may flow into the inconel vessel, with a possible dissipation of more than 4–5% of the total power input. Summarising, one may estimate that the LMP induces losses that amount to 15–35% of the total power input, largely due to the energy radiated as a consequence of the large impurity and hydrogen influx and to the halo currents through the vessel. These losses correspond to an enhancement of 5–13 V in the loop voltage out of the typical 30–35 V. The parallel losses to the wall connected to the LMP represent more than 10–15% of the total input power, but are not added to the other ones since they correspond to flows that would anyway reach the wall and are only prematurely intercepted.

With an alternative approach made in terms of helicity balance it has been shown that the interception of the field lines by the wall leads [14] to a direct loss of helicity corresponding to an enhancement of more than 7 V in the loop voltage, to be compared with the additive term of 8–10 V previously found from Z_{eff} measurements [10].

By removing the LMP with its severe plasma–wall interactions, the RFX discharges would benefit from a number of advantages: the removal of the direct losses, an overall reduction of the impurity content and therefore of the plasma resistivity with the associated helicity losses. Momentum losses associated with the LMP have not been considered here but could contribute to hamper the tendency of the plasma to rotate. The global magnetic diffusivity, that largely determines the RFP transport, could also improve by removing the LMP: in fact though it should not depend on the locking to the wall of the modes but only on the average magnetic energy of the perturbation [15], rotating modes should have smaller amplitudes.

References

[1] S. Itoh, K. Itoh and A. Fukuyama, J. Nucl. Mater. 220–222 (1995) 117.
[2] P. Sonato et al., J. Nucl. Mater. 227 (1996) 259.
[3] B.E. Chapman et al., Phys. Plasma 3 (1996) 709.
[4] F. D'Angelo and R. Paccagnella, The stochastic diffusion process in reversed-field pinch, Phys. Plasma 3 (1996), to be published.
[5] G. Fiksel et al., Phys. Rev. Lett. 27 (1994) 1028.
[6] S. Ortolani and D.D. Schnack, Magnetohydrodynamics of Plasma Relaxation (World Scientific, Singapore, 1993).
[7] V. Antoni et al., 22nd EPS Conf. on Plasma Phys. and Controlled Fusion, Bournemouth, Vol. IV (1995) p. 181.
[8] V. Antoni et al., First measurements of energy distribution of electrons on RFX edge plasma, Proc. 23rd EPS Conf., Kiev, to be published.
[9] L. Carraro et al., J. Nucl. Mater. 220 (1995) 646.
[10] L. Carraro et al., 22nd EPS Conf., Bournemouth (1995), Vol. III, p. 161.
[11] P.C. Stangeby and G.M. McCracken, Nucl. Fusion 30 (1990) 1225.
[12] F.C. Schuller, Plasma Phys. Controlled Fusion 37 (1995) A135.
[13] P. Sonato et al., these Proceedings, p. 982.
[14] B. Alper et al., Plasma Phys. Controlled Fusion 30 (1988) 843.
[15] F. D'Angelo and R. Paccagnella, Plasma Phys. Controlled Fusion 38 (1996) 313.